Thermochimica Acta, 42 (1980) 21—34
Elsevier Scientific Publishing Company, Amsterdam — Printed in Belgium

A CRADLE-GLASS AMPOULE SAMPLE CONTAINER FOR DIFFERENTIAL SCANNING CALORIMETRIC ANALYSIS

JAMES C. TOU * and LARRY F. WHITING

Analytical Laboratories, The Dow Chemical Company, Midland, MI 48640 (U.S.A.)

(Received 26 March 1980)

ABSTRACT

A sample container system was developed, which consists of a sealed micro-ampoule as the sample pressure vessel and a special ampoule cradle designed to optimize heat detection efficiency, reproducibility, baseline stability, and thermal responses. The heat detection efficiency and thermal responses of the sample container system were determined and compared to those of others. The reproducibility of heat measurements has been assessed using several common thermal standards and other chemicals. The interpretation of heat measurements by differential scanning calorimetry is also discussed.

INTRODUCTION

Because of the impact on the safety of manufacturing, transporting, storing and processing chemicals, calorimetric evaluations of thermally initiated chemical reactions have been attracting much attention and interest. This has led to the development of numerous new techniques [1]. Differential thermal analysis (DTA) [2] has been utilized in a routine manner in many laboratories for the semi-quantitative assessment of the thermal stability of chemicals. Recently, a differential scanning calorimeter (DSC) has been employed in the quantitative evaluation of not only heats of reaction but also reaction kinetics [3,4]. However, for a reaction system containing volatile components and/or releasing gaseous products, the conventional commerical aluminum sample pan suffers from rupture, which makes the quantitative evaluation of the DSC data very difficult. Furthermore, aluminum is known to be reactive toward many chemicals such as halogen-containing compounds, strong acids, etc. This often leads to erroneous results. Because of these drawbacks, several sample containers were developed for different types of applications. They are: sealed stainless steel cells [5], sealed glass capillary tube sample holders [6,7], Teflon® sealed metal cells [8—10], adhesive bonded aluminum pans [11], flat base flint glass ampoules [12] and the more recently developed sealed glass ampoule micro-reactors [13] and commercial Perkin-Elmer O-ring sealed stainless steel pans. Sample

* To whom correspondence should be addressed.

0040-6031/80/0000—0000/$ 02.50

holders containing polymeric materials are not suitable for calorimetric evaluation of many thermally initiated chemical reactions due to their temperature limitation.

The desirable characteristics of a sample container are: (1) being chemically inert; (2) having high calorimetric sensitivity; (3) providing quantitative data; (4) being simple in operation; (5) being capable of withstanding pressure build-up; (6) exhibiting fast thermal responses; and (7) giving stable daily baselines. In this paper, several different types of sample containers, based on the glass ampoule principle [13], are evaluated according to the above criteria, and the results are discussed.

RESULTS AND DISCUSSIONS

The melting behaviour of indium is often used in evaluating the performance of a DSC. The expected melting curve is shown in Fig. 1. The following quantities are utilized in the evaluation of various sample containers:

(1) the initial temperature, T_i, the intercept temperature, T_{int}, and the final temperature, T_f, for the temperature lagging information;

(2) the slope of the leading linear portion of the melting curve, $(T'—T_{int})/a$ (°C sec $mcal^{-1}$), for characterizing the thermal lag, where a is the energy response in $mcal\,sec^{-1}$ at temperature T' on the slope;

(3) the quantity, $(T_f—T_i)/h$ (°C sec $mcal^{-1}$), for defining peak broadening, where h is the peak energy response in mcal sec^{-1}; and

(4) the measured heat of melting, ΔH(mcal mg^{-1}), for evaluating heat transfer efficiency.

As described in the experimental section, the temperature scale and the sensitivity of the DSC employed were calibrated with indium in a commercial aluminum pan at a temperature scanning rate of 5°C min^{-1}. Therefore, for the various sample containers, all the quantities described above are

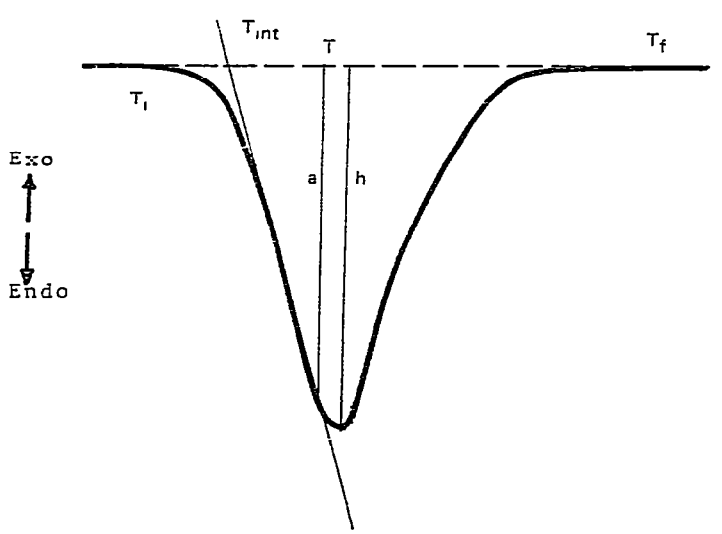

Fig. 1. A typical melting curve used for evaluation of thermal responses.

TABLE 1

The thermal responses of various sample containers

Technique	Scanning rate (°C min^{-1})	T_i (°C)	T_{int} (°C)	T_f (°C)	Thermal lag (°C sec $mcal^{-1}$)	Peak broadening (°C sec $mcal^{-1}$)	ΔH_m (mcal mg^{-1})
Al pan	5	156.8	157.0	160.0	0.551	1.96	6.85
	10	156.8	157.3	162.0	0.573	2.59	6.96
	20	157.6	158.0	166.5	0.563	3.65	7.07
	20 [a]	155.6	156.3	159.3	0.357	1.31	4.28
Chiu's [13] micro-reactor (Al)	5	159.3	160.0	171.5	5.78	37.0	4.86
	10	161.8	164.0	184.0	6.87	60.3	4.74
	20	166.3	168.0	193.3	10.3	78.75	3.10
P and E stainless steel pan	5	157.0	157.8	168.0	1.00	10.0	6.00
	10	157.8	158.5	179.5	1.26	17.9	6.05
	20	159.3	159.8	189.1	1.20	19.7	6.39
DTA [b]	5	154.3	154.6	160.5	13.4	21.7	0.67
	10	154.5	155.1	163.9	13.7	25.1	0.62
	20	156.1	156.8	168.2	13.7	25.0	0.58
Flattened base glass ampoule	5	157.8	158.0	164.8	3.37	8.96	5.98
	10	158.0	159.0	169.0	4.18	11.2	5.70
	20	159.3	160.3	177.3	4.31	13.7	5.91
Flattened base gold coated glass ampoule	5	157.5	158.0	163.2	5.20	16.1	2.63
	10	158.0	159.0	167.8	5.61	23.0	2.57
	20	159.0	160.0	173.0	5.72	23.4	2.72
Glass ampoule in double Al cradle	5	157.5	158.0	166.5	1.99	9.81	6.76
	10	158.0	158.8	173.0	2.15	13.2	6.79
	20	160.0	160.4	181.5	2.29	16.3	6.35
	10 [a]	156.8	157.5	164.8	1.39	6.34	4.94
Glass ampoule in single Al cradle	5	156.8	157.8	165.0	1.99	8.80	6.76
	10	157.8	159.3	173.5	2.35	14.9	6.69
	20	159.3	160.8	181.6	2.37	16.7	6.91
	10 [a]	156.8	157.8	163.3	1.34	4.94	4.64
Glass ampoule in double Ag cradle	5	157.8	158.3	168.0	2.40	12.5	6.92
	10	158.7	159.3	174.3	2.83	15.5	6.73
	20	160.0	161.0	184.5	3.07	21.4	6 48
	10 [a]	156.8	157.5	164.8	1.39	6.34	4.94
Glass ampoule in single Ag cradle	5	157.0	157.8	164.5	1.96	7.88	6.88
	10	157.8	158.5	171.0	2.13	11.2	6.88
	20	159.0	160.5	181.5	2.51	16.7	6.75

[a] He flow

[b] Separate instrument.

compared on a common basis. The thermal responses of the aluminum pan, Chiu's micro-reactor [13], Perkin-Elmer's stainless steel pan, DTA's capillary tube as well as the containers of different designs from the present work are shown in Table 1 as compared to the aluminum pan. The micro-reactor shows significant peak broadening and temperature and thermal lags. Only

44—71% of the heat of melting is detected, depending on the temperature scanning rate. The thermal lag of the Perkin-Elmer's stainless steel pan was found to be comparable to that of aluminum pans. However, the former shows pronounced tailing or a slower return to the baseline than the latter. This is reflected in the peak broadening measurements and the higher T_f, and is attributed to the large mass of the stainless steel pan.

Since the thermocouple pairs used in DTA and in DSC are different sets of Type J thermocouples, it is very difficult to compare the temperature measurements from the two techniques. However, the data shown in Table 1 clearly indicate the poor performance of DTA in thermal lag, peak broadening and heat transfer efficiency.

The use of a glass ampoule as a micro-reactor [13] is an excellent idea because of its chemical inertness. The poor thermal responses of this reactor reported above are believed to be due to the large mass of the ampoule holder. The simplest way to improve its thermal responses is to eliminate the ampoule holder and place the ampoule with its base flattened directly on the DSC sensor. The result is also shown in Table 1. As expected, both the ther-

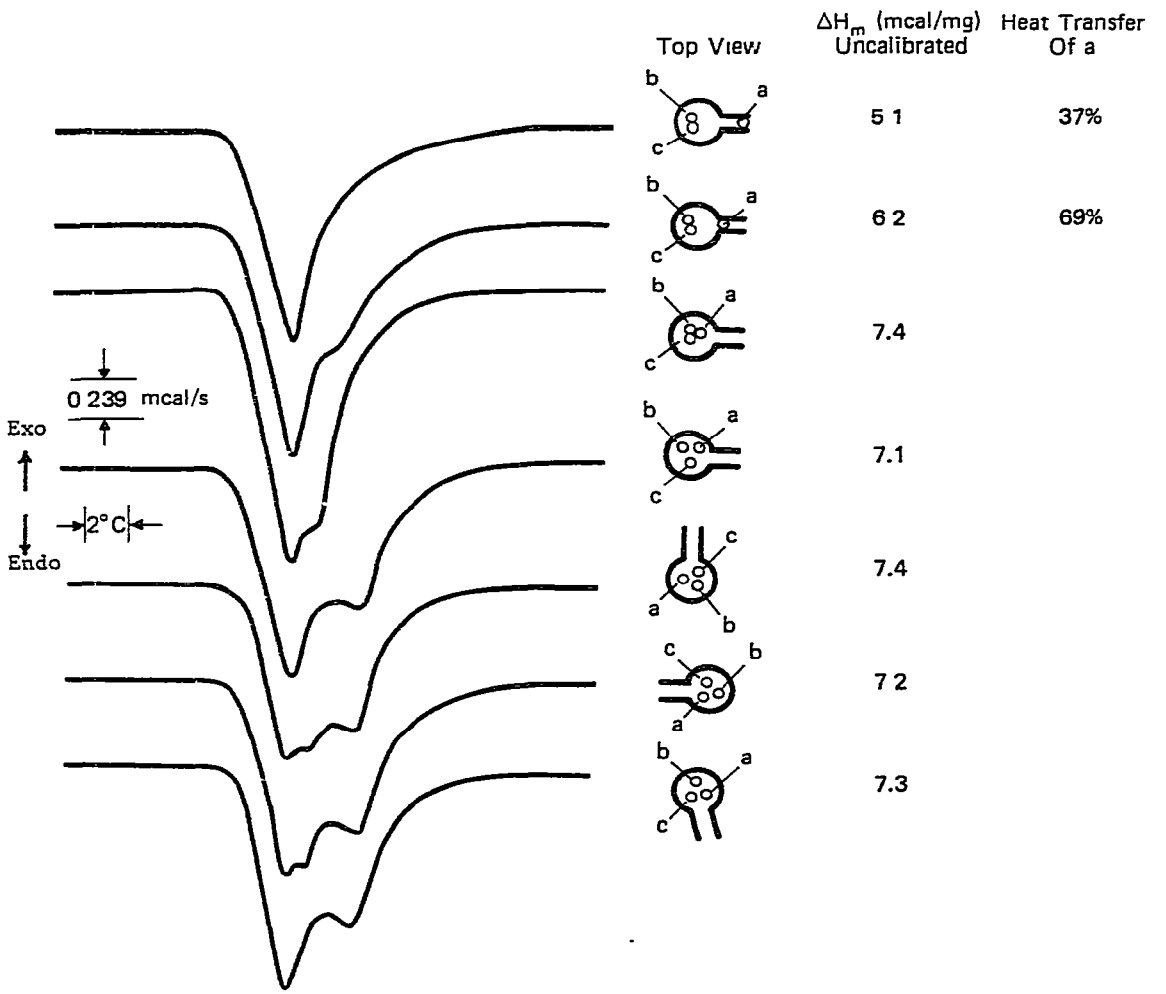

Fig. 2. The heat transfer characteristics of a flattened base glass ampoule.

mal responses and the heat transfer efficiency are significantly improved. As the data indicated, an attempt, made to further improve the heat transfer property with flattened base ampoule by coating it with gold, was not fruitful. Even though the technique is so simple, the most undesirable feature is the technical difficulty associated in flattening the base of the micro-ampoule evenly in order to have good thermal contact with the DSC sensor. If the base is not flattened evenly, the discrimination in sensing thermal activity taking place at different locations of the base is evident. This is shown in Fig. 2. Multiple peaks were observed for the melting of three different pieces of indium. The shape of the multiple peaks is dependent on how the flattened base ampoule was placed on the DSC sensor. Also shown in Fig. 2 is the heat transfer efficiency of the glass ampoule. The heat transfer was found to be only 37% when the sample was placed in the neck and improved to 69% when the sample was moved inward close to the opening of the neck. The efficiency reached ~100% when the sample was inside the ampoule. Another problem was the difficulty in controlling the thickness of the base during flattening. The effects of the thickness on heat transfer and the melting curve of indium are shown in Fig. 3. The thicker the base, the less efficient is the heat transfer and thus the broader is the melting curve.

Because of the drawbacks encountered with the flattened base glass ampoule discussed above, a light-weight silver or aluminum cradle was utilized as a heat transfer intermediate between the glass ampoule and the DSC sensor. Thermal responses were evaluated for two different arrangements, either

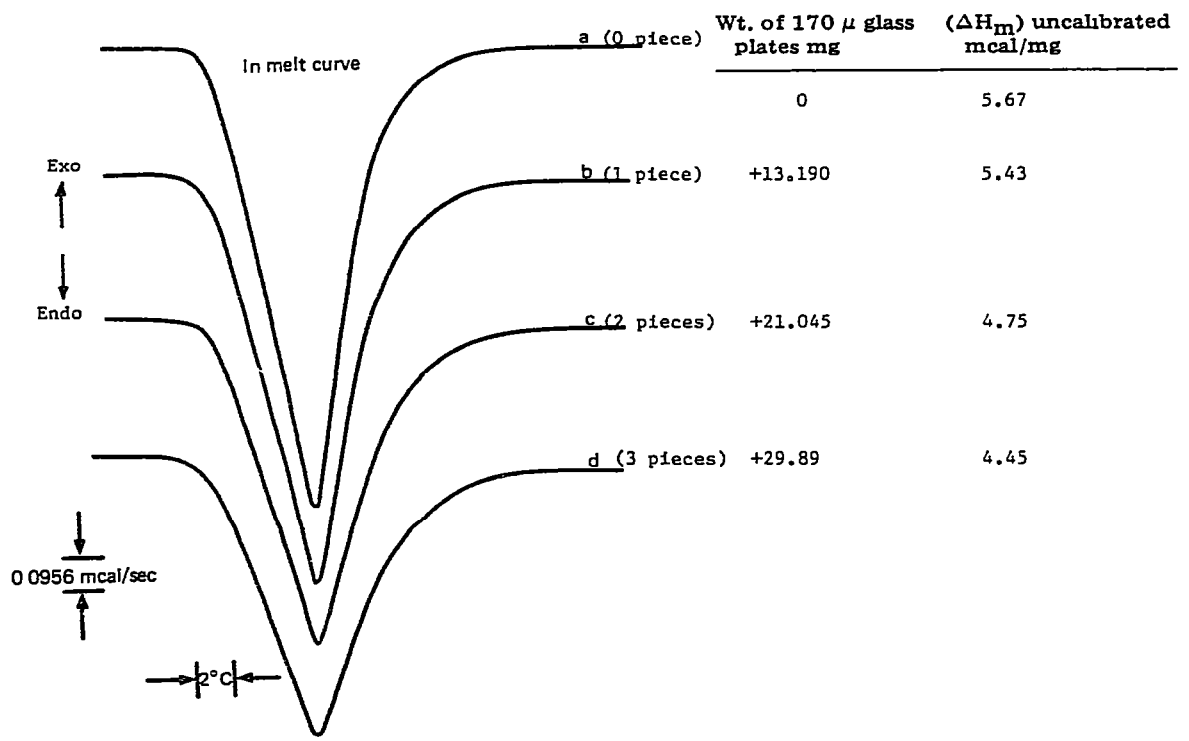

Fig. 3. The effect of the interface on the thermal response of a flattened base glass ampoule at 20°C min^{-1}.

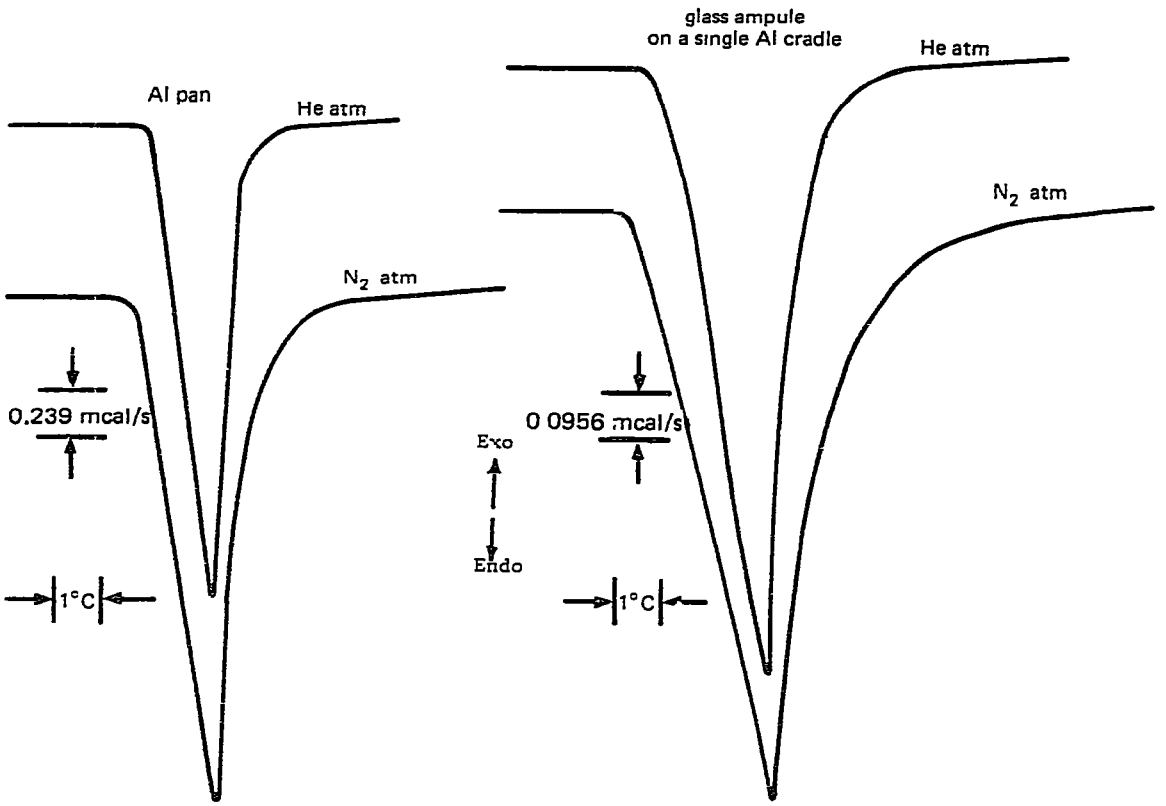

Fig. 4. The effect of atmosphere on the thermal responses of the indium melting curve

placing the glass ampoule on a single cradle, or sandwiching it between two cradles. The results are also shown in Table 1. It is clearly demonstrated that the present designs exhibited faster thermal responses than the other types of sample containers, and equal heat transfer efficiency to that of the conventional aluminum pan.

Since helium is one of the best heat conducting gases, the thermal responses were evaluated under the helium flow conditions. The data are shown in Table 1 and Fig. 4. In every case studied, significant improvement in thermal lag and the peak broadening was observed. The heat transfer efficiency was decreased, however, conceivably because part of the heat was transferred through the helium atmosphere instead of flowing between the two DSC sensors.

The thermal responses of a glass ampoule on a single aluminum cradle were also evaluated at various temperatures with use of tin and lead. The results shown in Table 2 indicate that both the temperature scale and the heats of melting are close to the reported literature values. In other words, the technique shows uniform responses in temperature and heat transfer efficiency. However, the data reveal a slight dependence of thermal lag and peak broadening on the samples.

It is also highly desirable to have the calorimetric system reach its thermal equilibrium as fast as possible. Shown in Fig. 5 are the dynamic responses

TABLE 2

Evaluation of thermal responses of glass ampoule on a single Al cradle at various temperatures

Sample	Experimental [a]							Literature	
	Scanning rate (°C min^{-1})	T_i (°C)	T_{int} (°C)	T_f (°C)	Thermal lag (°C sec mcal^{-1})	Peak broadening (°C sec mcal^{-1})	ΔH_m (mcal mg^{-1})	T_m (°C)	ΔH_m (mcal mg^{-1})
In	5	156 8	157.8	165.0	1.99	8.80	6.76	156.6	6.79
	10	157 8	159.3	173.5	2.35	14.9	6.69		
	20	159.3	160.8	181.6	2.37	16 7	6.91		
Tin	5	231.5	232 7	240.1	3.878	10.9	14.3	231.9	14.1
	10	232.2	233.5	245.1	3.21	11.2	15.1		
	20	234.0	236 4	255.6	3.57	23 4	14.3		
Pb	5	326 3	327.9	333.9	2.60	7.01	5.39	327.5	5.50
	10	326.7	328.2	340.6	2.65	9.56	5.46		
	20	328 2	328 9	349.0	3.01	12.20	5.30		

[a] The instrument was calibrated with In in an Al pan.

of several sample containers at three different temperature scanning rates. The conventional aluminum sample pans reach their thermal equilibrium much faster than other sample containers. The single- and double-cradle-glass ampoules also show an improved thermal response over the reported micro-reactor system [13]. The improved thermal response is demonstrated in Fig. 6 in a study of the thermal decomposition of di-*n*-butyl tin oxide. Several sharp endothermic transitions and exothermic reactions were observed. When the DSC was rescanned after the completion of the sample decomposition, an endothermic peak corresponding to the melting of tin was detected. It is obvious that tin was one of the thermal decomposition products.

Since the sensors are fixed in DSC, the baseline stability is expected to be better than the conventional DTA in routine analysis. When the single-cradle-ampoules were used, the baseline stability over a 2-week period with only vertical calorimetric offset adjustment is shown in Fig. 7. The data clearly reveal the stability of the daily baselines.

The linear response of the glass ampoule technique is demonstrated in Fig. 8 with the heat of melting of indium. The relative precision at the 95% confidence level was found to be ±14%.

The quantitative performance of the present cradle-glass ampoule technique was also evaluated for the thermal decomposition reactions of two selected samples, *N*-methyl-*N*-nitroso-*p*-toluenesulfonamide, commercially known as Diazald® and isopropyl peroxycarbonate in trichloroethylene. The former is a solid sample and the latter a 4.6% solution. Their DSC curves are shown in Figs. 9 and 10, respectively, along with the reproducibility data. In both cases, the reproducibility including sampling steps was found to be about ±14%, which is also consistent with that revealed in the response study described previously. Since isopropyl peroxycarbonate is unstable at

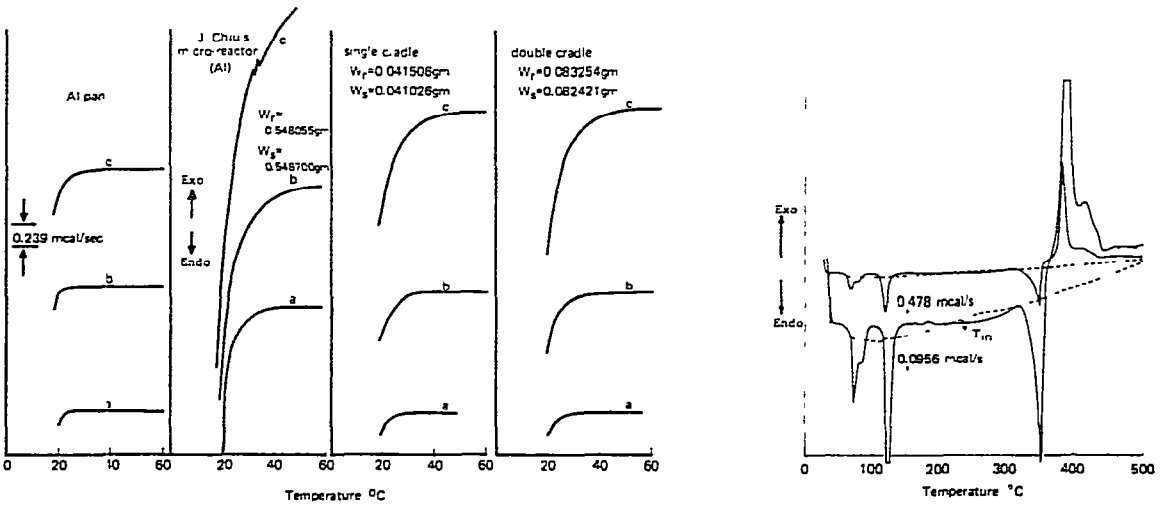

Fig 5 The dynamic thermal responses of various sample containers at scanning rates of (a) 5°C min^{-1}, (b) 10°C min^{-1}, and (c) 20°C min^{-1}.

Fig. 6. The DSC curves of di-*n*-butyl tin oxide at 20°C min^{-1}.

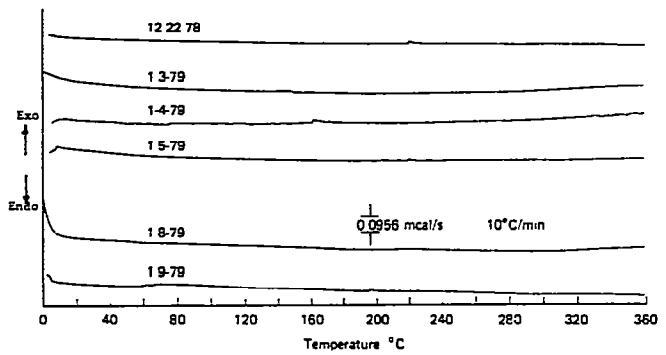

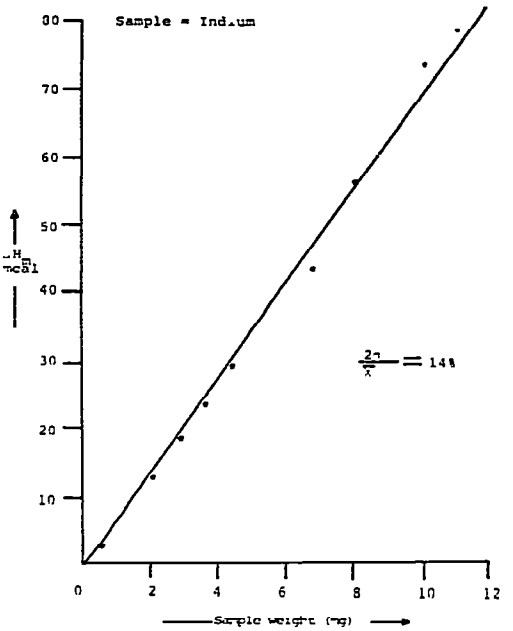

Fig. 7. Daily baseline reproducibility.

Fig. 8. Response linearity of glass ampoule technique.

room temperature and sensitive to moisture, an unknown amount may decompose during sample manipulation and therefore the heat of reaction obtained here may not be an accurate value. The data shown in Figs. 9 and 10 also reveal that the heats of decomposition within the experimental precision do not depend on whether single or double cradles are used. For simplicity in operation the single cradle is usually used.

Since a DSC experiment is carried out in a closed system and the sample ampoule presents a large void volume, when 3—4 mg of sample are loaded in a ~25 μl ampoule, the evaporation of liquid in the ampoule will cause a continuous endothermic shift of the DSC curve from the baseline. The shift results from the heat of vaporization and the change in heat capacity as a function of the sample temperature and is quite pronounced for liquid with high heat of evaporation and with heat capacity sensitive to temperature. Shown in Fig. 11 are three model calculations from the steam table [14], of the expected DSC curves for 0.5, 1.0 and 2.0 mg H_2O in a 25 μl ampoule, along with an experimental DSC curve for 0.581 mg H_2O in a 23.7 μl ampoule. The greater experimental initial shift from the baseline compared to the calculated one is attributed to the heat capacity of imbalanced mass between the reference and sample ampoules. Both the calculated and experimental curves show a return at an elevated temperature to the vicinity of the baseline and a levelling-off at higher temperature, indicating the completion of the evaporation process. The temperature at the point of return depends on the amount of sample loaded into the sample container. The larger the amount of sample, the higher is the temperature until the critical temperature is reached. This technique has been utilized as a means of deter-

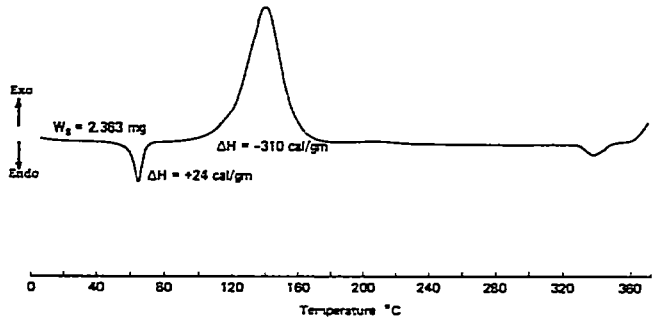

Method glass ampoule in single Al cradle

Amount loaded mg	ΔH_r mcal/mg
1 344	-290
1 047	-290
2.040	-310
2.363	-310
3.325	-255
1.260	-290
1 403	-290
1.587	-271
1 049	-310
1.290	-280
	-290 (1 ± 12%)

Method. glass ampoule in double Al cradle

1.342	-320
1.261	-300
1.258	-320

Fig. 9. The DSC curve of the thermal decomposition reaction of Diazald®.

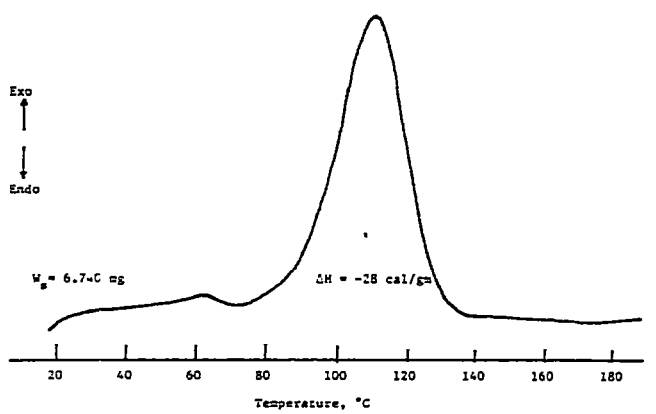

Method glass ampoule in single Al cradle

Amount loaded mg	ΔH_r mcal/mg
1 091	-28
6.740	-28
2.163	-27
3.096	-30
3.656	-24
3.776	-26
3.304	-30
3.416	-25
3.721	-28
3.341	-31
3.594	-29
3.690	-27
	-28 (1 ± 14%)

Method glass ampoule in double Al cradle

1 195	-25
1.387	-28

Fig. 10. The DSC curve of the thermal decomposition reaction of 4.6 st. % IPP in trichloroethylene.

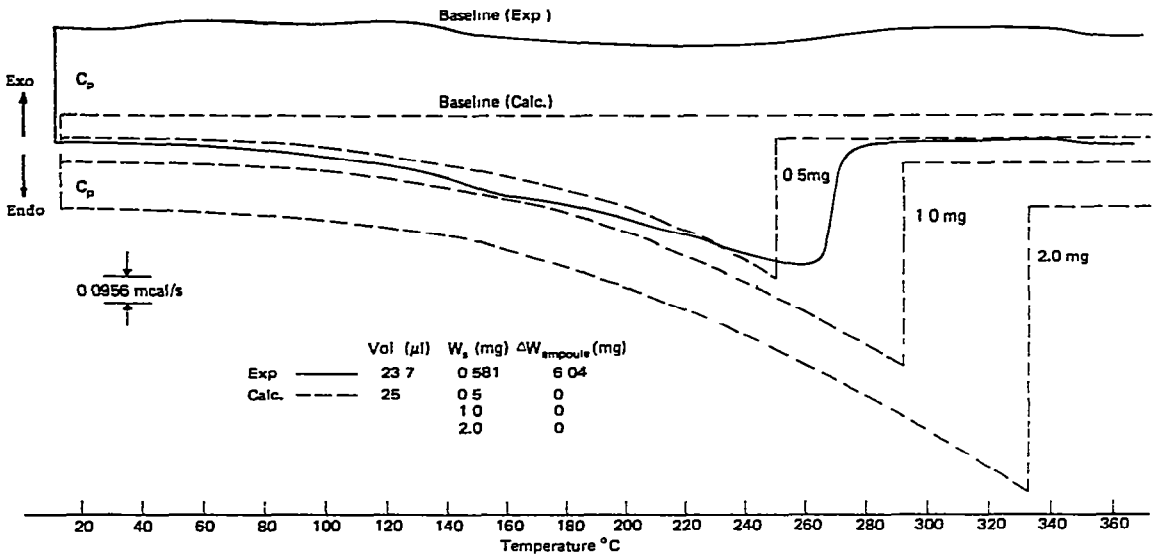

Fig. 11. The experimental and calculated DSC curves due to the evaporation of water.

mining critical temperatures [15], providing the sample container could withstand the critical pressures. As an illustrative case, an aqueous solution containing a reactant was subjected to a DSC study. The hypothetical DSC curve is shown in Fig. 12. The initial drop and the steady decline of the DSC

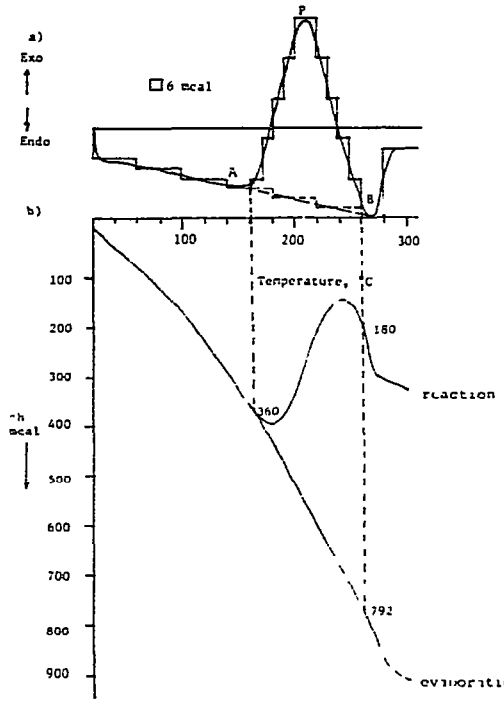

Fig. 12. A hypothetical DSC curve for an exothermic reaction of an aqueous solution (a) and the associated enthalpy diagram (b).

curve are mainly due to evaporation of H_2O. The reactant undergoes an exothermic reaction starting at 150°C and ending at 270°C. The evaporation of the solvent is completed around 280°C. The line AB represents the extension of the heat required for evaporation, assuming no reactant is present in the solution and the change in the heat capacities of the reactant and the product(s) are negligible. For simplicity, the DSC curve can also be approximately represented by a histogram. Since a DSC is an instrument for measuring effective heat capacity, ΔC_v, the heat or the enthalpy change, Δh (in cal g^{-1}), can be determined from

$$\Delta h = \int_{T_0}^{T_f} (\Delta C_v)_{exp}\, dT = \frac{60E\,\Delta q_s}{mH_r} \int_{T_0}^{T_f} \Delta y\, dt$$

where E is the cell constant, Δq_s the calorimetric sensitivity setting in cal(sec in)$^{-1}$, m the sample mass, H_r the temperature scanning rate, Δy the calorimetric deflection in inches from the baseline, T_0 and T_f the starting and final temperatures, respectively. The histographically calculated enthalpy changes as a function of final temperature are shown in Fig. 12b. Also shown in Fig. 12b is the enthalpy change of the solvent without reactant in it, by following line AB. Therefore the DSC sensible heat of reaction from 160 to 260°C is calculated to be 180 cal — 360 cal = —180 cal, and that of vaporization to be 792 cal — 360 cal = +432 cal. Conventionally, the heat of reaction is evaluated from the area bounded by the exothermic peak and the linearly interpolated baseline, i.e. the area APB shown in Fig. 12a. In this case, the heat of reaction is calculated to be —612 cal, which is exactly the difference between the DSC sensible heats of reaction and solvent vaporization —180 cal — (+432 cal) = —612 cal. In a DSC run, both the heat of vaporization and the changes in the heat capacities of reactant(s) and product(s) can complicate the curve shape, but the method for evaluating the heat of reaction remains the same as above. Brennan et al. [16] reported and discussed an improved procedure for isolating the enthalpy change from the heat capacity contributions. For a complex DSC curve resulting from a complex reaction system, finding a true baseline free from the contributions of heat capacity change and the heat of vaporization is a very difficult task. In such a case, a gross error may be involved in the determination of enthalpy changes.

The heat of reaction determined by a dynamic calorimetric method is often different from that determined by an isothermal calorimetric method. For a DSC curve represented in a histographic form, the heat, Δh_i, generated in a small section between T_i and T_{i+1} can be calculated to be

$$\Delta h_i = (f_{i+1} - f_i)\Delta H_i$$

where f_i and f_{i+1} are the fractions of reactants at T_i and T_{i+1}, respectively, and ΔH_i is the isothermal heat of reaction at T_i. The isothermal heat of reaction, ΔH_i, can be calculated from

$$\Delta H_i = \Delta H_0 + \int_{T_0}^{T_f} \Delta C_v\, dt$$

where ΔC_v is the net change in the heat capacities of the reactant(s) and the product(s) and ΔH_0 is the known heat of reaction at T_0. The heat of reaction, ΔH, determined from DSC, is thus

$$\Delta H = \Sigma \Delta h_i = \Sigma(f_{i+1} - f_i)\,\Delta H_0 + \Sigma(f_{i+1} - f_i) \int_{T_0}^{T_f} \Delta C_v \, dt = \Delta H_0 + \int_0^1 \int_{T_0}^{T_f} \Delta C_v \, dT \, df$$

Therefore the heats of reaction determined by the isothermal and dynamic calorimetric methods are the same only if $\Delta C_v = 0$. This requirement is not usually met. Therefore, care should be taken in the interpretation of the heats of reaction by the above mentioned methods. Even for a first-order reaction, the fraction of reactant reacted, f, is a complex function of temperature, temperature scanning rate and the kinetic parameters of the reaction, which makes the integration difficult [17].

EXPERIMENTAL

All of the experiments were carried out in a DuPont model 910 differential scanning calorimeter or a standard DuPont DTA cell driven by a DuPont

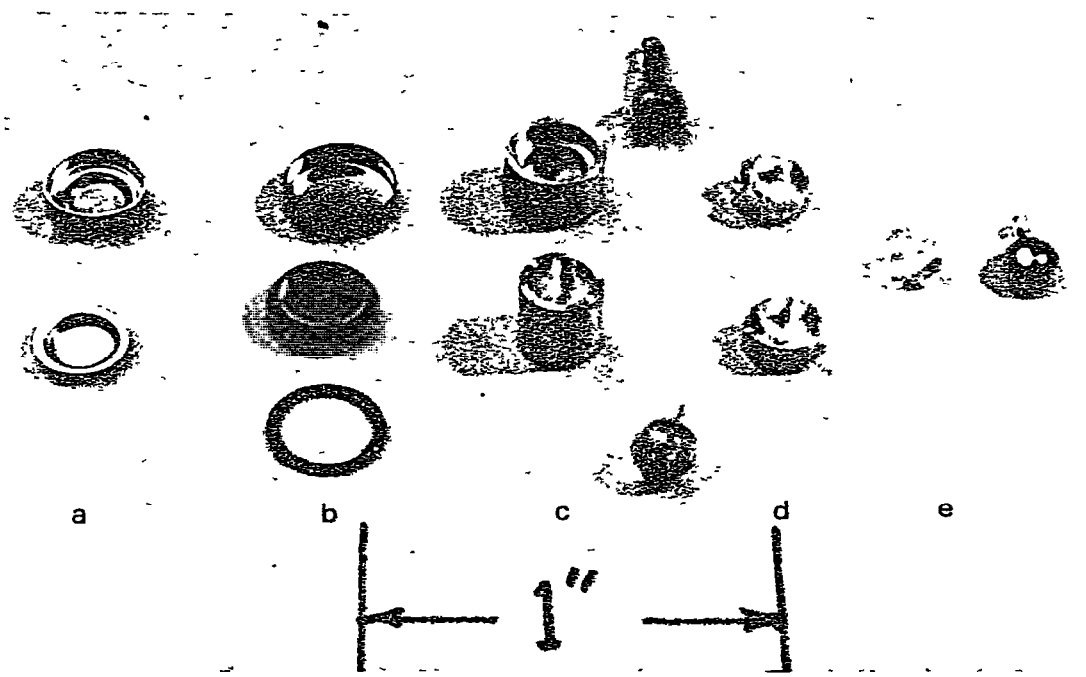

Fig. 13. Various DSC sample containers evaluated. (a) Commercial aluminum sample pan, (b) Perkin-Elmer O-ring sealed stainless pan; (c) glass ampoule micro-reactors; (d) cradle-glass ampoule sample container, and (e) flattened base glass ampoules: gold coated (right) non-coated (left).

model 990 temperature programmer. The temperature scale and the calorimetric sensitivity of the DSC unit was calibrated with indium in the commercial aluminum pan at a scanning rate of 5°C min^{-1}. The sample containers evaluated in this work are shown in Fig. 13. Two types of glass ampoules were employed in this study. The one purchased from Kontes of Illinois, Evanston, IL (K-897020) has a thicker wall and therefore withstands higher pressure (~1800 psi vs. ~500 psi) than that from Wilmad Glass Co., Inc. (No. 529). The breakage of the thicker wall ampoule, due to the internal pressure build-up from sample evaporation and/or decomposition, can cause damage to the DSC cell base, while the potential damage from the thinner wall is significantly less severe. All of the thermal responses reported in this paper were measured with the thicker walled ampoule. An automatic sealing device was constructed based on the principle of liquid-nitrogen cooling and micro-torch sealing. Reproducible sealing at ~2 mm above the neck position was achieved with the use of this device. Whenever understanding of the chemistry of the thermal reaction is desirable, the reaction can be quenched at any selected temperature. The ampoule can be crushed in a sealed vial and the reaction contents dissolved in a solvent for subsequent chromatographic and/or spectroscopic analysis.

ACKNOWLEDGEMENTS

The authors would like to express their sincere appreciation to R. Tait, P. Patterson and R. Bushong for experimental assistance, to E. Hallberg and H. Morrison for their design and construction of the automatic glass ampoule sealing device, and J. Kochanny and G. Crable for their valuable comments.

REFERENCES

1 D.I. Townsend and J.C. Tou, Thermochim. Acta, 37 (1980) 1 and references cited therein.
2 ASTM Method E 537-76.
3 A.A. Duswalt, Thermochim. Acta, 8 (1974) 57 and references therein.
4 T. Ozawa, J Therm. Anal., 2 (1970) 301.
5 C.J.H. Schouteten, S. Bakker, B. Klazema and A.J. Pennings, Anal. Chem., 49 (1977) 522.
6 W.W. Wendlandt, Anal. Chim. Acta, 49 (1970) 188.
7 H.W. Hoyer, A.V. Santoro and E.J. Barrett, J. Polym. Sci., Part A-1, 6 (1968) 1033.
8 F.E. Freeberg and T.G. Alleman, Anal. Chem., 38 (1966) 1806.
9 K.E.J. Barrett and H.R. Thomas, J. Polym. Sci. Part A-1, 7 (1969) 2621.
10 V.W. Knappe, G. Nachtrab and G. Weber, Angew. Makromol. Chem., 18 (1971) 169.
11 K. Horie, I. Mitta and H. Kambe, J. Polymer. Sci., Part A-1, 6 (1968) 2663.
12 G.R. Taylor, G.E. Dunn and W.B. Easterbrook, Anal. Chim. Acta, 53 (1971) 452.
13 J. Chiu, Thermochim. Acta, 26 (1978) 57.
14 R.H. Perry and C.H. Chilton (Eds.), Chemical Engineering Handbook, 5th edn., McGraw-Hill, New York, Sect. 3-206.
15 G. Hentz, Thermochim. Acta, 20 (1977) 27.
16 W.P. Brennan, B. Miller and J. Whitwell, Ind. Eng. Chem., 8 (1969) 314.
17 L.F. Whiting and P.W. Carr, Anal. Chem., 50 (1978) 1997 and references therein.